*Materials Research*. 2023; 26: e20220467
DOI: https://doi.org/10.1590/1980-5373-MR-2022-0467

# Investigations on Tribological Behaviour of ZK60A Mg alloy–TiN Composites Synthesized via Powder Metallurgy Technique

***H. Saravanan[a*], M. Ravichandran[b], Dhinakaran Veeman[c], S.V. Alagarsamy[a]***

*[a]Mahath Amma Institute of Engineering and Technology, Department of Mechanical Engineering, Pudukkottai, 622 101, Tamil Nadu, India.*
*[b]K. Ramakrishnan College of Engineering, Trichy, 621 112, Tamil Nadu, India.*
*[c]Chennai Institute of Technology, Centre for Additive Manufacturing, Chennai, 620 109, Tamil Nadu, India.*

Received: November 01, 2022; Revised: March 03, 2023; Accepted: March 30, 2023

The development in current manufacturing technology entails better wear resistance materials. Inthis study, ZK60A Mg alloy matrix composites reinforced with x wt.% (x = 0, 4, 8 and 12 wt.%) of TiN powders are developed through powder metallurgy (PM) route. The tribological behaviour of the composites under dry sliding conditions was estimated using Pin-on-disc instrument. The influence of the control parameters such as wt.% of TiN, applied load , sliding velocity and sliding distance on the wear rate and co-efficient of friction were analysed using Taguchi coupled grey relational approach GRA and $L_{16}$ orthogonal array is selected for performing design of experiments. The lowest WR of 0.01147 $mm^3$/m and 0.2446 COF formed at 12 wt.% of 'R', 9.81 N of 'P', 5.24 m/s of 'V' and 1000 m of 'D'. From Analysis of variance (ANOVA), the wt.% of TiN powder (P = 82.68%) was observed as a primary factor controlling the WR and COF of composites. Finally, confirmation trials were performed to validate the results. SEM examination ensures homogeneous disbursement of TiN powders in the matrix alloy. Addition of reinforcement results in increase in density and porosity. The higher hardness observed at 12wt.% TiN incorporated Mg alloy composite.

**Keywords:** *ZK60A Mg alloy, TiN, PM technique, Tribological behaviour, GR approach.*

## 1. Introduction

Metal matrix composites (MMCs) has increasing demand day by day due to promising advanced properties for newer and as well as for recent technological innovation applications which entail high performance lighter weight materials. Nowadays, there has been a significant research intention for Mg alloys owing to their low densities, high specific strength, and good damping capacities which attract several applications in aerospace, structural, defence, automation and transportation industries[1,2]. On the contrary, the low wear and corrosion resistance of these alloys, prevents them from being used in a larger variety of applications[3]. Various researches have exhibits that the wear behaviour of Mg based MMCs can be enhanced by inclusion of hard or self lubricating ceramic as reinforcement particles[4]. The inclusion of ceramic particles such as SiC, TiC, SiO2, TiN, TiB2, MoS2, B4C, Al2O3, and addition of Gr particles has shown characteristics improvement in the tribological properties of Mg based composites and materializes convinced morphological changes[5,6].

Amongst the literature available pertaining to Mg related composite works, TiN ceramic particulates have supremacy over other reinforcements for the proven sake that it has good ductility, strength, hardness and increment in wear resistance. Several methods have been employed during the past years for developing MMCs, among all these methods, PM technique possesses numerous advantages for producing composites[7]. The PM technique can obtain materials with a high volume fraction of ceramic reinforcement and can gain uniformity in the distribution of reinforcement at a lower manufacturing temperature itself which makes it superior than conventional stir casting technique[8]. Shuai Sun et al.[9] studied the properties of AZ31 Mg alloy composites incorporated with vanadium ($V_p$) particle through PM route. They observed that the higher hardness value was achieved at AZ31-2.5 wt.% $V_p$ composite. Ali Ercetin and Danil Yurievich observed that the addition of $Al_2O_3$ reinforcement significantly improved the hardness of Mg2Zn matrix alloy composites. The microstructure ensures the existence of $Al_2O_3$ particle homogeneously distributed at the grain boundaries[10]. Aatthisugan et al.[11] investigated the wear behaviour of $B_4C$ and Gr particle reinforced AZ91D Mg matrix composites and they reported that the inclusion of both reinforcements drastically improves the wear resistance. Narayanasamy and Selvakumar described the mechanical and wear behaviour of Gr and $MoS_2$ reinforced Mg matrix composites developed through PM route. They stated that the hardness and wear resistance drastically enhanced in $MoS_2$ addition rather than Gr[12]. Dash et al.[13] stated the wear and mechanical properties of TiC incorporated with Mg alloy AZ91D matrix composites and they concluded that an increase in TiC content significantly improved the tensile strength, hardness and compression strength in Mg alloy. They also reported that the specific wear rate (SWR) decreases when the load increases from 10-50 N due to the inclusion of TiC in Mg alloy. Meher et al.[14] studied the

*e-mail: mailtohsaran@gmail.com

hardness and wear behaviour of various proportions of $TiB_2$ filled Mg RZ5 alloy composite and they revealed that the higher hardness was obtained at 8wt.% $TiB_2$ addition of Mg alloy composite. Similarly, the wear loss of proposed composites drastically reduced by adding $TiB_2$ content and the worn surfaces indicated the groove and delamination occurred in the composite specimen. Sunu Surendran and Gnanavelbabu[15] reported that the WR notably decreased in AZ91D Mg alloy composites reinforced with TiC, $TiB_2$ and TiN ceramic particles. It has also been observed the formation of delamination and abrasion wear mechanism on the specimen surface by SEM micrograph. Satish and Satish[16] described the impact of SiC and $Al_2O_3$ particle on hardness and wear resistance of Mg matrix composites developed through PM route. They noticed that the inclusion of both reinforcements considerably enhances the hardness and resistance to wear. It has also been found that increase in 'P' rising the WR[16]. Mehra et al.[17] optimized the wear parameters on RZ5-TiC composite using Taguchi method and they concluded that the minimum weight loss was obtained at 10 N of load, 700 m of sliding distance and 10 wt.% of TiC content, respectively. ANOVA result revealed that 'D' and wt.% of TiC content were a dominant factor for weight loss. Sathish et al.[18] studied the effect of parameters on SWR and COF for the Mg-Al-Ti composite developed by disintegrated melt deposition technique. They described that 'P' and 'V' has the primary noteworthy factor for COF and SWR with a contribution of 39.72% and 82.90%, respectively. Selvam et al.[19] studied the wear behaviour of ZnO nano particle reinforced Mg matrix composite synthesized via PM technique. They noted that WR drastically increased when an increasing in 'P' and 'V'. Meanwhile, an increase in 'D' decreasing the COF. Lim et al.[20] explored the wear behaviour of Mg-SiC composites and they found that proposed composites exhibit 15-30% improvement in wear resistance due to addition of reinforcement have obtained greater load bearing capacity. Mahesh et al.[21] examined the wear behaviour of TiN reinforced Al matrix composites fabricated through PM technique and reported that the wear resistance of composite considerably increased with the increase in TiN reinforcement. They also noticed that the 'P' increasing the wear resistance decreased significantly. Sathish et al.[22] optimized the wear parameters of $2.5B_4C$ filled Mg-5.6Ti-3Al composite using Taguchi technique and they understood that 'P' has the prime important factor for control the WR followed by 'V'. Tarasasanka et al.[23] employed the grey relational analysis for optimizing the dry sliding wear behaviour of nano $Al_2O_3$ particle reinforced Mg AZ91E composite. They determined that the 'V' at 1 m/s, 'D' of 500 m and 'P' of 10 N gives the less WR and COF. Shen et al.[24] examined the wear behaviour of nanoscale SiC incorporated Mg AZ31 alloy composite under dry sliding conditions. They concluded that WR gradually increased with the increase in 'V' or 'P'. However, the less WR achieved at higher 'P' conditions for the produced composites.

From a thorough review of the literature, we concluded that predicting the tribological behaviour of Mg MMCs is a challenging process since it depends on a number of variables, including 'R', 'P', 'V', and 'D'. Therefore, a detailed statistical evaluation is essential to determining the best tribological behaviour of Mg MMCs. Additionally, a comprehensive review of the literature indicated that no experimental or statistical work has been done to examine the tribological behaviour of ZK60A Mg alloy-TiN composites produced via PM method. In order to forecast the tribological behaviour of TiN particle reinforced ZK60A Mg alloy composites Taguchi's integrated grey relational approach were employed.

## 2. Experimental Details

### *2.1. Synthesize of composites*

In the present investigation, ZK60A Mg alloy (Zn-5.5, Zr-0.45 and Mg-remaining) powder was chosen as matrix material which was procured from Loba Cheme Pvt. Limited., Mumbai. Titanium Nitride (TiN) powder with a particle size of 50µm was utilized as reinforcement supplied by Alfa Aesar Private Limited. The powder metallurgy (PM) route was employed to synthesize the Mg alloy matrix composites by adding different proportion (0, 4, 8, and 12 wt.%) of TiN particles. The powders were first dried for 1 hr at roughly 100°C in an oven, and then they were mixed for at least 6 hr in a planetary tumbler mixer revolving at 300 rpm and utilizing stainless steel balls with a diameter of 10 mm for 10:1 BPR weight ratio. After mixing, the powders were cold compacted in a cylindrical die at a pressure of 600 MPa to obtain a 20 mm diameter and 10 mm height of the specimen. Finally, the green compacts were sintered under argon gas atmosphere for 1 hr at 450°C in a tubular furnace. Further, the composite specimens were permitted to cool down inside the room temperature. The process sequence of experimental work is shown in Figure 1.

### *2.2. Testing of composites*

SEM (Vega3 Tescan) was used to observe the microstructure of the proposed composites. Before the observations, the composite samples were polished by disc polishing machine. The experimental density of the composites was measured by using the Archimedes principles as per ASTM: B962-08 standards[25] The theoretical density was calculated using rule of mixture and the porosity of the sintered composite has also been calculated. A Rockwell hardness tester was used to test the composites' hardness. The specimen was prepared in accordance with ASTM standards, and the hardness test using a ball indenter with a 100 kg force. The composite specimen underwent three different hardness tests, with the average results being taken into account. The tribological behavior like a WR and COF for the synthesized Mg-TiN composites was estimated by performing the dry sliding wear test using a pin-on-disc (Wear & Friction Monitor TR-20, Ducom) instrument. The test specimens were created using 10 mm diameter and 30 mm length measurements. The counter disc was made of hardened EN-31 steel plate, which has a hardness of 60 HRC. The disc and the test specimens were polished with fine emery sheets and cleaned with acetone solutions prior to the wear test. The wear tests were carried out as per $L_{16}$ orthogonal design by choosing four control variables[26], each at four levels as shown in Table 1. An end of the test, the mass loss of the specimen was estimated by weighing instrument with an accuracy of 0.0001g, respectively. The WR and COF were calculated by applying standard equations[27] and the results are depicted in Table 2.

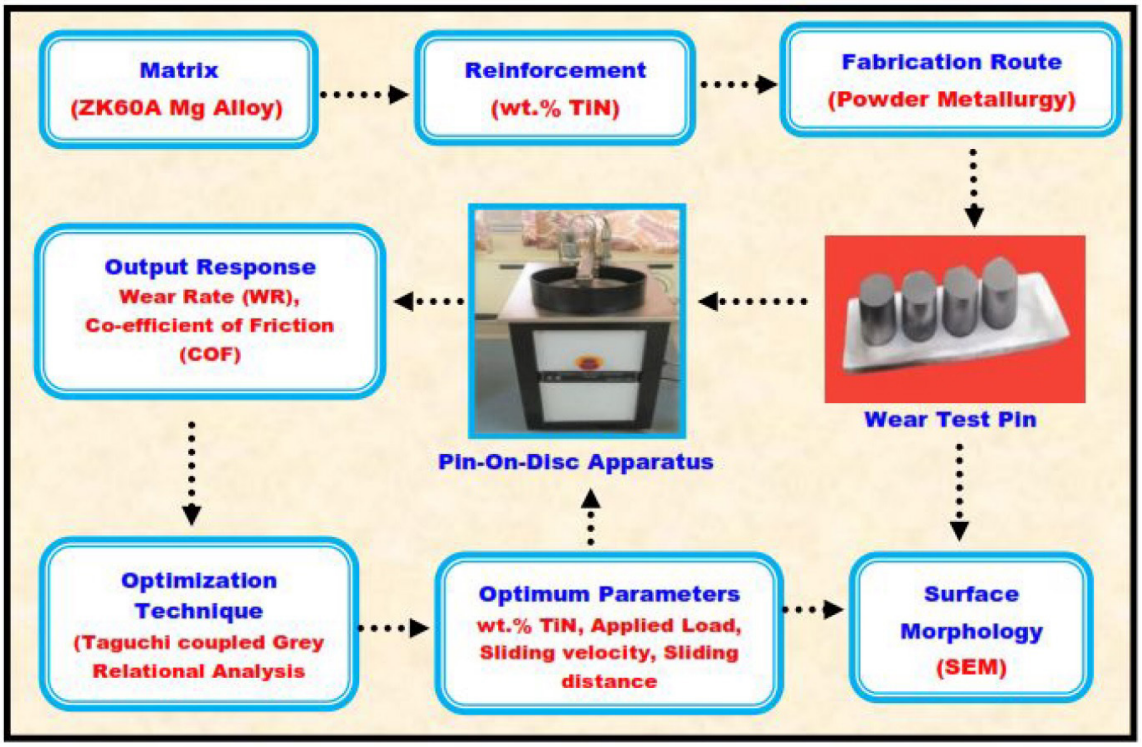


**Figure 1.** Layout of present experimental work.

**Table 1.** Control parameters and their levels.

| Notation | Control Parameters | Units | Parameters at Four Level | | | |
|---|---|---|---|---|---|---|
| | | | 1 | 2 | 3 | 4 |
| R | TiN | wt.% | 0 | 4 | 8 | 12 |
| P | Applied load | N | 9.81 | 19.62 | 29.43 | 39.24 |
| V | Sliding velocity | m/s | 1.30 | 2.62 | 3.92 | 5.24 |
| D | Sliding distance | m | 500 | 1000 | 1500 | 2000 |

**Table 2.** L16 design layout: Input parameters and output responses.

| Ex. No | TiN (wt.%) | Applied load (N) | Sliding velocity (m/s) | Sliding distance (m) | Wear rate ($mm^3$ /m) | COF (μ) |
|---|---|---|---|---|---|---|
| 1 | 0 | 9.81 | 1.3 | 500 | 0.02235 | 0.3874 |
| 2 | 0 | 19.62 | 2.62 | 1000 | 0.02607 | 0.4179 |
| 3 | 0 | 29.43 | 3.92 | 1500 | 0.03352 | 0.4689 |
| 4 | 0 | 39.24 | 5.24 | 2000 | 0.05587 | 0.5122 |
| 5 | 4 | 9.81 | 2.62 | 1500 | 0.02183 | 0.3670 |
| 6 | 4 | 19.62 | 1.3 | 2000 | 0.03125 | 0.3823 |
| 7 | 4 | 29.43 | 5.24 | 500 | 0.02344 | 0.4349 |
| 8 | 4 | 39.24 | 3.92 | 1000 | 0.02778 | 0.4740 |
| 9 | 8 | 9.81 | 3.92 | 2000 | 0.01301 | 0.3160 |
| 10 | 8 | 19.62 | 5.24 | 1500 | 0.01463 | 0.2758 |
| 11 | 8 | 29.43 | 1.3 | 1000 | 0.01839 | 0.3024 |
| 12 | 8 | 39.24 | 2.62 | 500 | 0.01951 | 0.3772 |
| 13 | 12 | 9.81 | 5.24 | 1000 | 0.01147 | 0.2446 |
| 14 | 12 | 19.62 | 3.92 | 500 | 0.00917 | 0.2582 |
| 15 | 12 | 29.43 | 2.62 | 2000 | 0.01223 | 0.2650 |
| 16 | 12 | 39.24 | 1.3 | 1500 | 0.01835 | 0.2881 |

### *2.3. Grey relational approach (GRA)*

Prof. Deng developed the grey relational approach in 1982. It has shown to be a useful tool for dealing with incomplete, suspect, and inadequate primitive data in system models. The term "grey relation" refers to an incomplete data relationship. In order to solve complicated problems involving the interactions between the multiple objective features, GRA is often used[28]. In this analysis, the prediction of complex multi-performance criteria can be transformed into a single grey relational grade (GRG). In this study, GRA was utilized to find the optimal conditions of parameters for achieving lesser WR and COF for the TiN reinforced ZK60A Mg alloy composites while dry sliding wear test. The following procedures were used to accomplish a grey relational analysis:

**Step 1:** By using Taguchi method, signal to noise (SN) ratio was estimated for the responses. Here, we need less WR and COF for the synthesized composites, then smaller-the-better SN ratio has been selected and the relation is given in Equation 1,

$$S/N\ ratio = -10\log_{10}(1/n)\sum_{k=1}^{n} Y_{ij}{}^{2} \quad (1)$$

Where n – No. of trials, Yij – estimated response, where i = 1, 2, 3…..n; j = 1, 2, 3…….k.

**Step 2:** Prior to using the grey relation theory to analyze the responses, normalization of the data is necessary. Here, the measured responses were scaled from 0 to 1 after being normalized. The response is considered as "smaller-the-better" then the original order is normalized by using Equation 2.

$$Z_i^{*}(k) = \frac{\max Z_i(k) - Z_i(k)}{\max Z_i(k) - \min Z_i(k)}, \quad (2)$$

where, $Z_i^{*}$(k) - the values after the normalizing, $Z_i$(k) – the original value of responses, max $Z_i$(k) – the higher value of $Z_i$(k), min $Z_i$(k) –the lower value of $Z_i$(k) for the k$^{th}$ response. Table 3 depicted the estimated SN ratios and normalized SN ratios for the WR and COF.

**Step 3:** The normalized SN ratios were used to obtain the grey relational coefficient (GRC) $\xi_i(k)$ for the responses by using Equation 3.

$$\xi_i(k) = \frac{\Delta\min + \zeta \cdot \Delta\max}{\Delta_{0i}(k) + \zeta \cdot \Delta\max} \quad (3)$$

**Step 4:** The grey relational grade (GRG) was estimated by averaging the GRC for each response and the Equation 4 was used.

$$\gamma_i = \frac{1}{m}\sum_{k=1}^{m} \xi_i(k) \quad (4)$$

where, $\gamma_i$ - the GRG for the i$^{th}$ trial, $\xi_i$ - the GRC and m – no. of responses. The estimated GRC and GRG with order in rank are depicted in Table 4.

Figure 2 depicts the rank plot for GRG with all the experiments performed while dry sliding wear process. In Figure 2, x –axis represented the experiment number and y-axis showed the obtained GRG. From the plot, we can take the optimal conditions of control parameters on the responses. It was evident that experiment number 13 has produced the highest GRG (0.955166), which corresponds to the best set of optimal parameters (R = 12 wt.%, P = 9.81 N, V = 5.24 m/s, and D = 1000 m) for achieving the lowest WR and COF during the dry sliding process of ZK60A Mg alloy composites.

**Table 3.** Estimated SN ratios and normalized SN ratios.

| Ex. No | SN ratios | | Normalized SN ratios | |
|---|---|---|---|---|
| | WR (dB) | COF (dB) | WR (dB) | COF (dB) |
| 1 | 33.01445 | 8.236808 | 0.717773 | 0.466368 |
| 2 | 31.67718 | 7.578553 | 0.638116 | 0.352392 |
| 3 | 29.49392 | 6.578395 | 0.478587 | 0.161809 |
| 4 | 25.05643 | 5.811209 | 0 | 0.000000 |
| 5 | 33.21893 | 8.706679 | 0.728908 | 0.542601 |
| 6 | 30.10300 | 8.351914 | 0.527195 | 0.485426 |
| 7 | 32.60085 | 7.232212 | 0.694433 | 0.288864 |
| 8 | 31.12536 | 6.484433 | 0.601499 | 0.142750 |
| 9 | 37.71445 | 10.00626 | 0.917773 | 0.733184 |
| 10 | 36.69511 | 11.18811 | 0.883084 | 0.883408 |
| 11 | 34.70837 | 10.38836 | 0.80257 | 0.784006 |
| 12 | 34.19485 | 8.468566 | 0.778587 | 0.504484 |
| 13 | 38.80873 | 12.23087 | 0.950749 | 1.000000 |
| 14 | 40.75261 | 11.76088 | 1 | 0.949178 |
| 15 | 38.25147 | 11.53508 | 0.934475 | 0.923767 |
| 16 | 34.72728 | 10.80913 | 0.803426 | 0.837444 |

**Table 4.** Calculated deviation sequences, GRC and GRG.

| Ex. No | Deviation sequence | | GRC | | GRG |
|---|---|---|---|---|---|
| | WR | COF | WR | COF | |
| 1 | 0.282227 | 0.533632 | 0.639201 | 0.483731 | 0.561466 |
| 2 | 0.361884 | 0.647608 | 0.580124 | 0.435689 | 0.507906 |
| 3 | 0.521413 | 0.838191 | 0.489518 | 0.373639 | 0.431578 |
| 4 | 1 | 1.000000 | 0.333333 | 0.333333 | 0.333333 |
| 5 | 0.271092 | 0.457399 | 0.648431 | 0.522248 | 0.585340 |
| 6 | 0.472805 | 0.514574 | 0.513978 | 0.492818 | 0.503398 |
| 7 | 0.305567 | 0.711136 | 0.620680 | 0.412836 | 0.516758 |
| 8 | 0.398501 | 0.857250 | 0.556482 | 0.368392 | 0.462437 |
| 9 | 0.082227 | 0.266816 | 0.858772 | 0.652047 | 0.755409 |
| 10 | 0.116916 | 0.116592 | 0.810482 | 0.810909 | 0.810696 |
| 11 | 0.19743 | 0.215994 | 0.716917 | 0.698330 | 0.707624 |
| 12 | 0.221413 | 0.495516 | 0.693084 | 0.502252 | 0.597668 |
| 13 | 0.049251 | 0.000000 | 0.910331 | 1.000000 | 0.955166 |
| 14 | 0 | 0.050822 | 1.000000 | 0.907734 | 0.953867 |
| 15 | 0.065525 | 0.076233 | 0.884135 | 0.867704 | 0.875920 |
| 16 | 0.196574 | 0.162556 | 0.717799 | 0.754653 | 0.736226 |

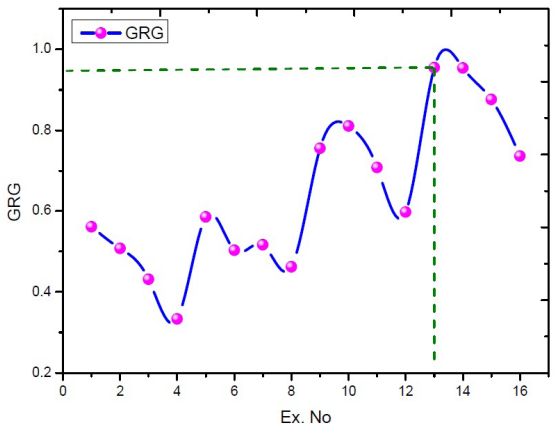


**Figure 2.** Rank plot for GRG.

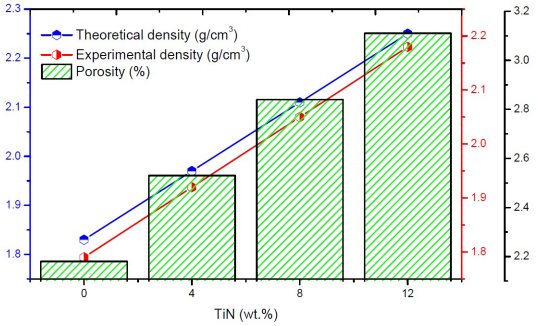


**Figure 3.** Density and porosity of Mg-TiN composites.

## 3. Results and Discussion

### *3.1. Density and porosity measurements*

The results of density measurements of the produced pure Mg Alloy and Mg Alloy -TiN composites are depictied in Figure 3. A marginal increase in the experimental density was identified with the addition of up to 12 Wt. % TiNreinforcements. The trend of decrease in relative densities with increase in TiN content is due to progressive increase in the presence of micro-porosities. Further the porosity of synthesised material increases with increase in TiN particles and well within the limits reported. It has been noted that the minimum porosity was found at Mg ZK60A and maximum porosity is observed for 12 wt% addition of TiN reinforcement.

### *3.2. SEM morphology*

Figure 4a-d depicts the SEM micrographs, which illustrates the pure alloy and synthesized composites. The microstructure consists of two phases, dark and white as shown in Figure 4b-d. The dark zone indicates the base alloy and white zone represent the reinforcement content. In Figure 4a display the microstructure of pure alloy, it can be ensured the non existence of reinforcement and also it shows some pores or voids formation in a few regions. As shown in Figure 4b-d, the SEM micrographs of composites confirm a homogeneous dispersion of TiN particles in the base alloy. However, a slight amount of agglomeration of reinforcement particles seen in some places, thus create the porosity in the fabricated composites. In general, Mg was good wettability element, which enhances the strong interfacial bonding between the reinforcement and matrix[29].

### *3.3. Effect of TiN on Hardness*

Figure 5 depicts the Rockwell hardness values of TiN reinforced ZK60A Mg alloy composites. It can be ascertained that the pure Mg alloy has a hardness (38 HRB) that is much lower than composites. It's clearly seen that the hardness significantly improvements when the inclusion of TiN particles. Moreover, an increase in wt.% of TiN content increasing the hardness. The higher hardness value (65.8 HRB) obtained at 12wt.% TiN reinforcement addition of composite.

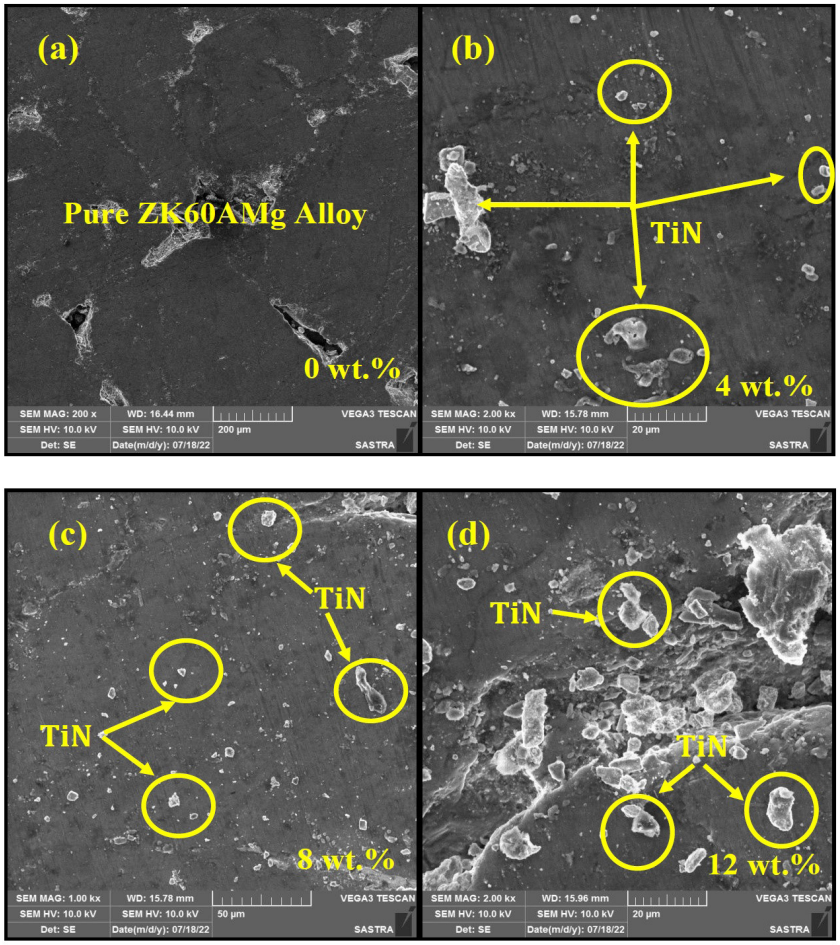


**Figure 4.** SEM images of sintered ZK60A Mg alloy-TiN composites (a) 0wt. %, (b) 4wt. %, (c) 8 wt. %, and (d) 12wt. %.

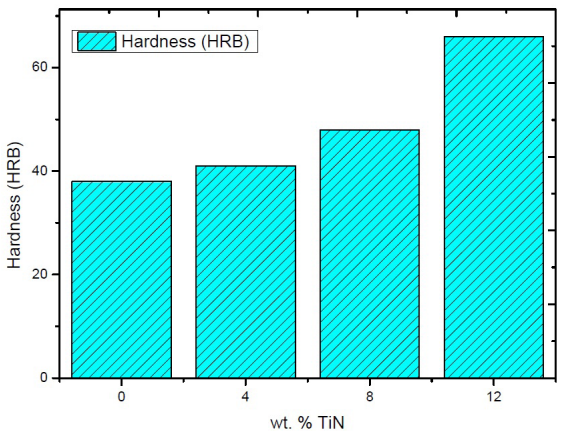


**Figure 5.** Hardness of sintered ZK60A Mg alloy-TiN composites.

This was because homogeneous distributions of TiN particle refine the grain structure and resist local plastic deformation of the base alloy during indentation. In addition, the hardness of TiN particles are relatively higher as a result TiN produced higher hardness.

### *3.4. Analysis of parameters on GRG*

Figure 6 shows the effect of control parameters, namely reinforcement (R), applied load (L), sliding velocity (V) and sliding distance (D) on multi-response tribological behavior of Mg-TiN composites while dry sliding wear test. From Figure 6a, it is clearly seen that the GRG improved when an increase in TiN content from 0 to 12wt.%. The less WR and COF are achieved at ZK60A Mg alloy-12wt.% TiN composite. An increase in TiN particles enhances the hard surface of the matrix alloy thus lead to increase the wear resistance. By considering the 'P' (Figure 6b), the lower level of 'P' (9.81 N) produces less WR and COF for the synthesized composites. Moreover, with an increase in 'P', the WR and COF gradually increased at higher value. Usually, the produced WR and COF mostly depend on 'P'. In this investigation, 'P' is primary significant factor for affecting the responses. Similarly, the WR and COF linearly increased when an increase in 'V' as shown in Figure 6c. The initial level of 'V' (1.30 m/s) produces low WR and COF, after that it will slightly increase at maximum level. In Figure 6d reveals that the lower 'D' gives minimum WR and COF for the tested composites. However, the maximum WR and COF developed at higher 'D'.

The mean value of GRG in relation to each level of control parameters is shown in Table 5. The table shows that the higher value of GRG is comparable to the control parameters' optimal outcome. As per the Table 5, the wt.% of TiN content at level $R_4$ (12 wt.%), applied load at level $P_1$ (9.81 N), sliding velocity at level $V_4$ (5.24 m/s) and sliding distance at level $D_2$ (1000 m) given the lower WR and COF for the fabricated AZ60A Mg alloy-TiN composites during the dry sliding wear test. Additionally, it has been stated that the consequence of control parameters on responses by using delta value. Based on the delta value, rank 1 represented as a primary noteworthy factor followed by others. In Table 5 clearly depicts that the 'R' has the most significant factor for affecting the WR and COF, next by 'P'. But, the 'V' and 'D' has an insignificant factor on responses. The similar results were previously observed by Sai Ram et al.[30] while a dry sliding wear test for Mg AZ91E composites.

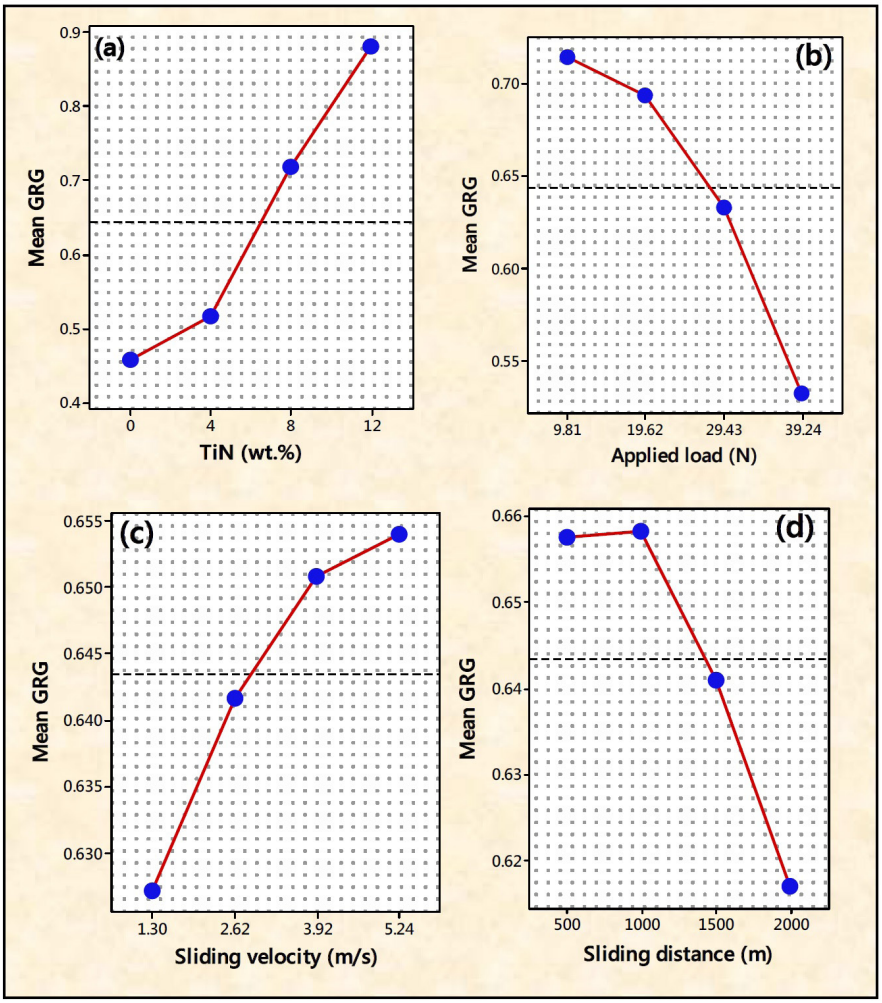


**Figure 6.** Main effect plot for GRG.

**Table 5.** Mean table for GRG.

| Level | R (wt.%) | P (N) | V (m/s) | D (m) |
|---|---|---|---|---|
| 1 | 0.4586 | 0.7143* | 0.6272 | 0.6574 |
| 2 | 0.5170 | 0.6940 | 0.6417 | 0.6583* |
| 3 | 0.7178 | 0.6330 | 0.6508 | 0.6410 |
| 4 | 0.8803* | 0.5324 | 0.6540* | 0.6170 |
| Delta | 0.4217 | 0.1819 | 0.0268 | 0.0413 |
| Rank | 1 | 2 | 4 | 3 |
| Average mean GRG = 0.643424 | | | | |

'*'optimum level

### *3.5. Influence of control parameters on WR*

Figures 7a-f illustrate the contour effect of control parameters, namely 'R', 'P', 'V', and 'D' on WR for the TiN particulate filled ZK60A Mg alloy composites. In Figure 7a reveals the interaction of 'R' and 'P' on WR of the tested composites. It can be seen that the WR gradually decreased with an increasing trend in TiN reinforcement because of the less WR (<0.015 $mm^3$ /m) of tested composites obtained at 12 wt.% TiN content. Therefore, an increase in 'P' from 10 N to 35 N the same is occurring at the same time. So that, the higher WR (> 0.05 $mm^3$/m) is obtained by pure Mg alloy at maximum 'P' condition. In Figure 7b depicts the interaction of 'R' versus 'V' on WR. From the Fig, it can be noticed that the minimum WR (0.015 $mm^3$/m) is achieved at higher 'V' condition by 12 wt.% of TiN reinforced composite. Based on the results (Table 6), 'V' has an insignificant factor in the responses. However, the WR gradually increases with an increase in 'V' by unreinforced alloy. Figure 7c reveals the effect of 'R' versus 'D' on WR. It was observed that the higher 'D' produced more WR for the pure matrix alloy. Furthermore, the WR slightly decreased with an increase in TiN content. The reason is that, the reinforcement of TiN particles improved the hard surface on the proposed composites thus results in enhanced the wear resistance.

In Figure 7d illustrates the impact of 'P' versus 'V' on WR. It can be explored that the less WR (<0.015 $mm^3$/m) has attained from 10 N to 20 N of 'P' with maximum 'V' condition. Meanwhile, the WR increased when an increase in 'P' at maximum level. Similarly, the moderate WR (0.027-0.033 $mm^3$/m) has produced at 20 N of 'P' with 2.5 m/s of 'V', respectively. In Figure 7e display the effect of 'P' with 'D' on WR. It clearly noted that the less

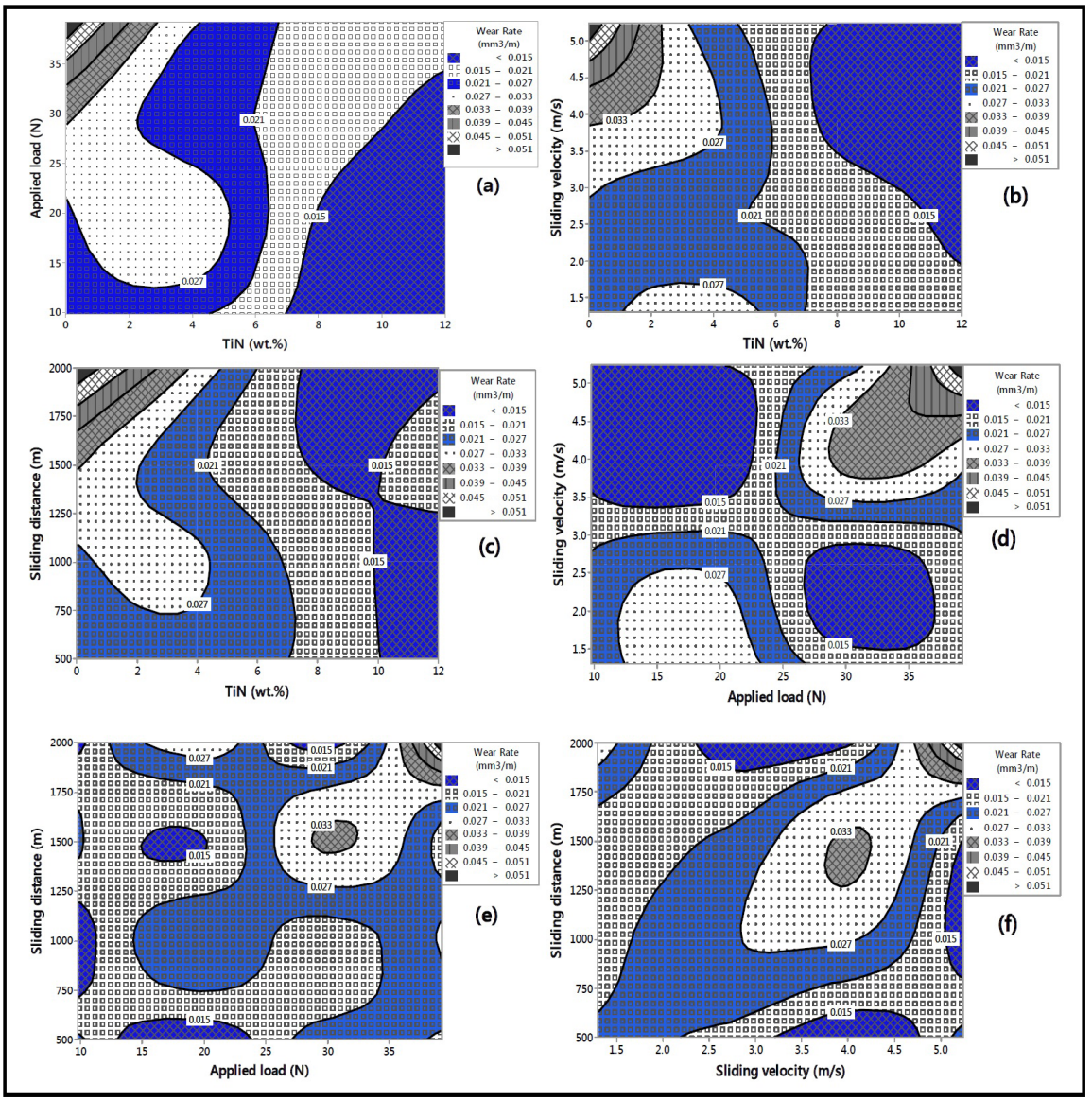


**Figure 7.** Contour plot for WR with respect to control parameters.

WR (0.015 $mm^3/m$) obtained at 20 N of 'P' with initial value of 'D'. Furthermore, an increase in 'P' with 'D' increases the WR. Hence, the higher WR (0.051 $mm^3/m$) has produced at 40 N of 'P' with 2000 m of 'D', respectively. From Figure 7f demonstrate the influence of 'V' with 'D' on the WR of reinforced composite. It clearly reveals that the greater WR from 0.045 to 0.051 $mm^3/m$ make at higher 'V' with longer 'D'. However, the WR gradually reduced when setting of 'V' from 1.30 m/s to 3.92 m/s.

### *3.6. Influence of control parameters on COF*

Figure 8a-f illustrates the contour graph for COF with respect to control parameters, namely 'R', 'P', 'V', and 'D'. In Figure 8a shows the influence of TiN (wt.%) with 'P' on COF for the tested ZK60A Mg alloy composites. It can be noted that low COF (<0.25) produced at 12 wt.% TiN reinforced composite with initial 'P' of 10 N. Moreover, with an increase in 'P' COF gradually improved[31].

**Table 6.** ANOVA for GRG.

| Factors | DF | Seq. SS | Adj. SS | Adj. MS | F | P | P (%) |
|---|---|---|---|---|---|---|---|
| R (wt.%) | 3 | 0.447219 | 0.447219 | 0.149073 | 60.78 | 0.003 | 82.68 |
| P (N) | 3 | 0.080066 | 0.080066 | 0.026689 | 10.88 | 0.040 | 14.80 |
| V (m/s) | 3 | 0.001733 | 0.001733 | 0.000578 | 0.24 | 0.867 | 0.32 |
| D (m) | 3 | 0.004483 | 0.004483 | 0.001494 | 0.61 | 0.653 | 0.82 |
| Errors | 3 | 0.007358 | 0.007358 | 0.002453 | -- | -- | 1.36 |
| Total | 15 | 0.540859 | -- | -- | -- | -- | 100 |
| S = 0.0495252; R-Sq = 98.64% ; R-Sq(adj) = 93.20% | | | | | | | |

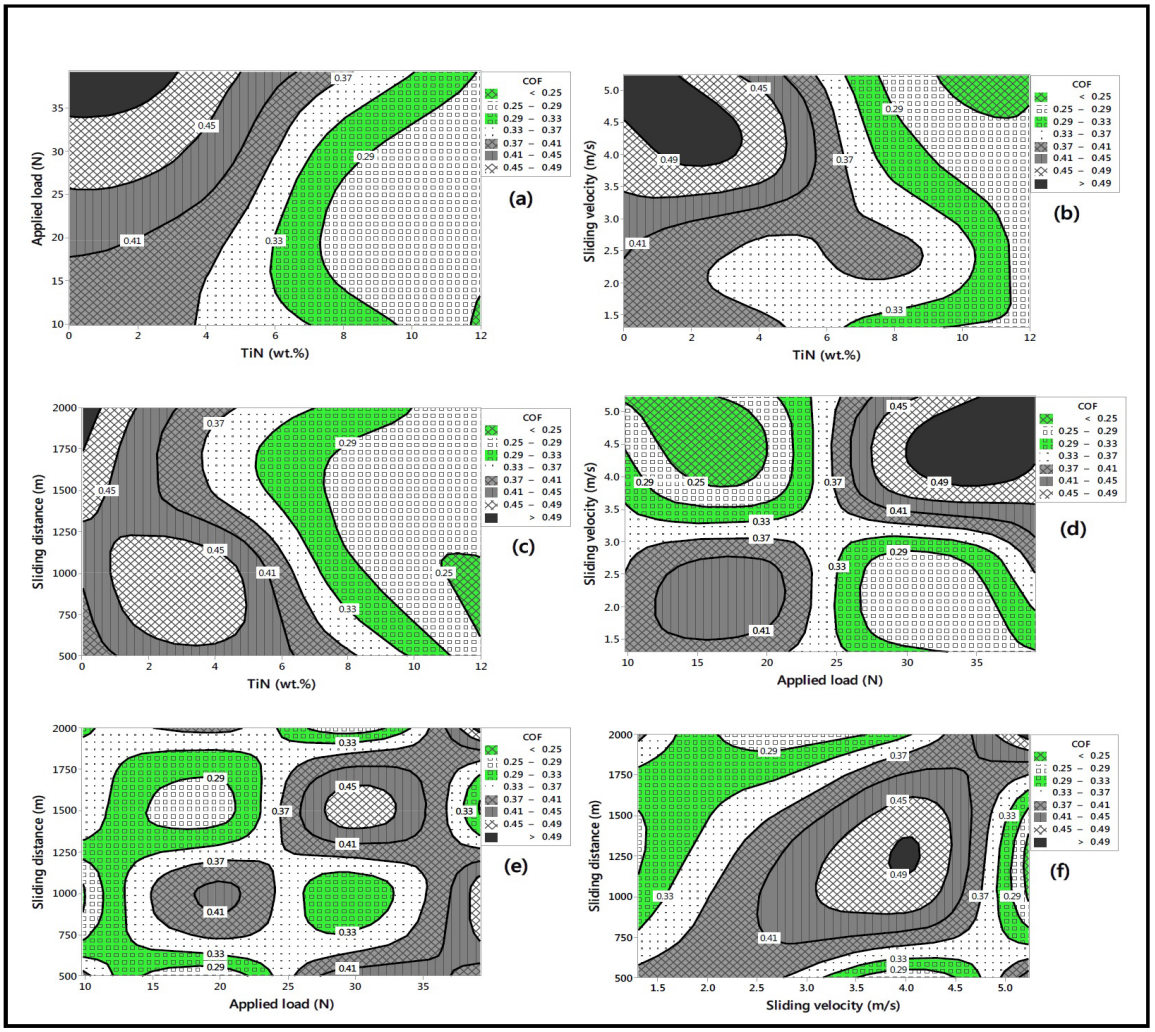


**Figure 8.** Contour plot for COF with respect to control parameters.

The maximum COF (<0.49) made in the pure Mg alloy by considering a high level of 'P'. In Figure 8b illustrates the contour graph for COF with respect to 'R' and 'V'. It can be noticed that the maximum COF (0.49) seen at 5.24 m/s of 'V' and 0 wt.% of TiN composite. However, 12 wt.% TiN filled composite with high 'V' (5.24 m/s) produces less COF (<0.25). Meanwhile, a moderate 'V' gives an average COF (0.41) by 4 wt.% TiN composite. The interaction effect of 'R' versus 'D' on COF is shown in Figure 8c, it can be stated that the minimum COF (<0.25) attained that 12 wt.% of TiN reinforced composite with 1000 m 'D'. Meanwhile, with an increasing in 'D' increases the COF of reinforced Mg alloy. Furthermore, the COF gradually decreases from 0.45 to 0.33 when an increase in TiN content. Figure 8d depicts the effect of 'P' with 'V' on COF, it can be observed that the initial 'P' with higher 'V' gives lower COF (0.25). Furthermore, with an increase in 'P' gradually enhances the COF at a high level of 'V'. So that, the maximum COF (0.49) has done at high 'P' (39.24 N) and 'V' (5.24 m/s), respectively. It was also noted that the middle level of 'P' and 'V' develop moderate COF. The influence of 'P' versus 'D' on COF is displayed in Figure 8e. From the graph, it was noticed that the minimum COF of 0.29 has produced at 20 N of 'P' with 1500 m of 'D'. Meanwhile, the COF increases with increase in 'P'. The 'D' has considered as an insignificant factor, then the 'P'. Hence, 'D' doe's not affect the COF. Figure 8f shows the contour graph for COF with respect to 'V' and 'D', it clearly noted that 'V' of 3.92 m/s with 'D' at 1000 m develop high COF (0.49). Meanwhile, the lower level of 'D' produces less COF (0.29) at 3.92 m/s of 'V'.

### *3.7. ANOVA Analysis*

ANOVA is a statistical approach which can be used to determine the influence of parameters on the responses and it has also revealed the contribution percentage of each parameter[32]. In the study, ANOVA was efficiently applied to find out the order of influencing parameters, namely 'R', 'P', 'V', and 'D' on WR and COF for the synthesized Mg-TiN composites while dry sliding wear test. The result of ANOVA for GRG is shown in Table 6. Based on the F-ratio and P-value (Table 6), the influence of parameters can be identified at 95% CI. It has been proved that the wt. % of TiN (R) was the primary eminent factor, followed by an applied load (P) because of the F-ratio of 'R' (F - 60.78) and 'P' (F – 10.88) are incredibly larger than the tabulated F-value ($F_{0.05,\ 3,\ 15}$ = 3.29), and also the P-value of those parameters is less than 0.05, respectively. It was also found that the percentage contribution of 'R' is 82.68% and 'P' is 14.80%. The 'V' and 'D' are considered as insignificant factors with contributions are 0.32% and 0.82%, only. The similar observations were reported to the dry sliding wear process of ZnO reinforced Al-Zn-Mg-Cu alloy composites[33]. Figure 9 depicts the residual plots for GRG and it was explored that the residuals are to be evenly placed along the straight line at 95% CI.

### *3.8. Confirmation experiment*

After selecting the most suitable range of control parameters, a confirmatory test was run to ensure that the analysis was accurate. The appropriate level of control parameters was utilized in this confirmation test to confirm the response attributes of the dry sliding process of ZK60A Mg alloy-TiN composites. The predicted value of GRG was computed by using Equation 5.

$$\beta_{pre} = \beta_m + \sum_{k=1}^{n} (\beta_i - \beta_m) \tag{5}$$

where, $\beta_{pre}$- predicted GRG, $\beta_m$- total mean GRG, $\beta_i$- is GRG at the optimum level parameters and k- number of control parameters involved. Table 7 depicts the predicted and experimental values of the GRG and it was revealed that they are reasonably similar. The value of GRG significantly improved to 0.342023 from the initial level to the optimum level. Hence, this makes it feasible to use this approach for choosing the appropriate parameters for numerous performance criteria.

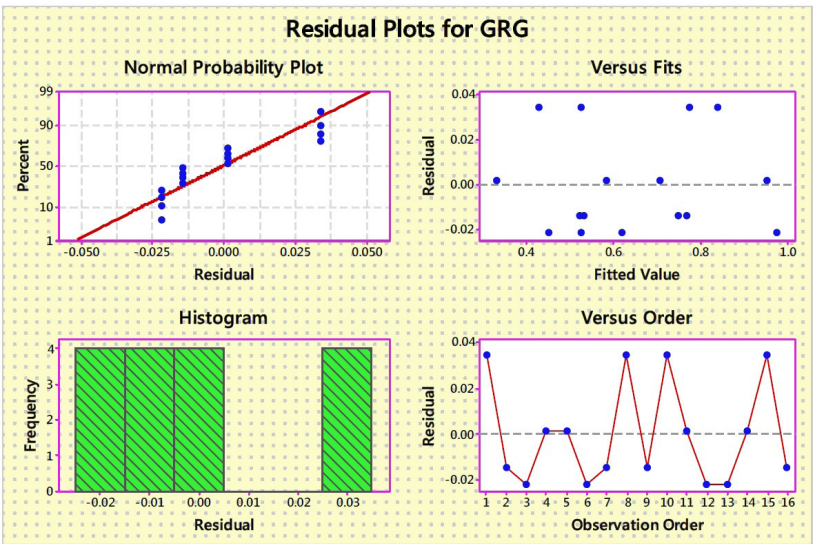


**Figure 9.** Residual plot for GRG.

### *3.9. Worn surface morphology*

Figure 10a-d shows the SEM micrographs of worn surface of ZK60A Mg base alloy and 4, 8 and 12 wt.% TiN reinforced composites with a parameter condition of 'P' at 9.81 N, 'V' of 5.24 m/s and 'D' of 1000 m. The worn surface morphology revealed the formation of plough, delamination, long grooves and oxide layer along with wear debris. In Figure 10a shows the initiation of grooves and delamination on the worn surface of pure alloy. Moreover, some pits and debris are shown in the worn surface. This was happened to soft nature of Mg alloy doesn't resist against the load. The micro-cutting, plough and small grooves creation on the surface are clearly noticed by 4 wt.% TiN reinforced composite (Figure 10b). This was due to the asperities of disc surface penetrate into the specimen surface. In Figure 10c, the worn surface showed in deep grooves along the sliding direction due to plastic deformation by abrasion. During sliding, the TiN particle was smeared and formed a thin oxide film layer, which protect the specimen surface from the wear loss. The similar observation was earlier reported[11]. In Figure 10d exhibits the some fine grooves and formation of smooth surfaces on the surface of the 12 wt.% TiN reinforced composite. Due to increasing trend of TiN content produce mechanical mixed layer (MML) on the surface thus improve the wear resistance for the synthesized composite.

**Table 7.** Results of confirmation experiment.

| Responses / Level | Initial | Predicted | Experimental |
|---|---|---|---|
| | $R_1P_1V_1D_1$ | $R_4P_1V_4D_2$ | $R_4P_1V_4D_2$ |
| WR ($mm^3/m$) | 0.02235 | - | 0.01147 |
| COF (μ) | 0.3874 | - | 0.2446 |
| GRG | 0.561466 | 0.976628 | 0.955166 |
| Improvement of GRG = 0.3937 | | | |

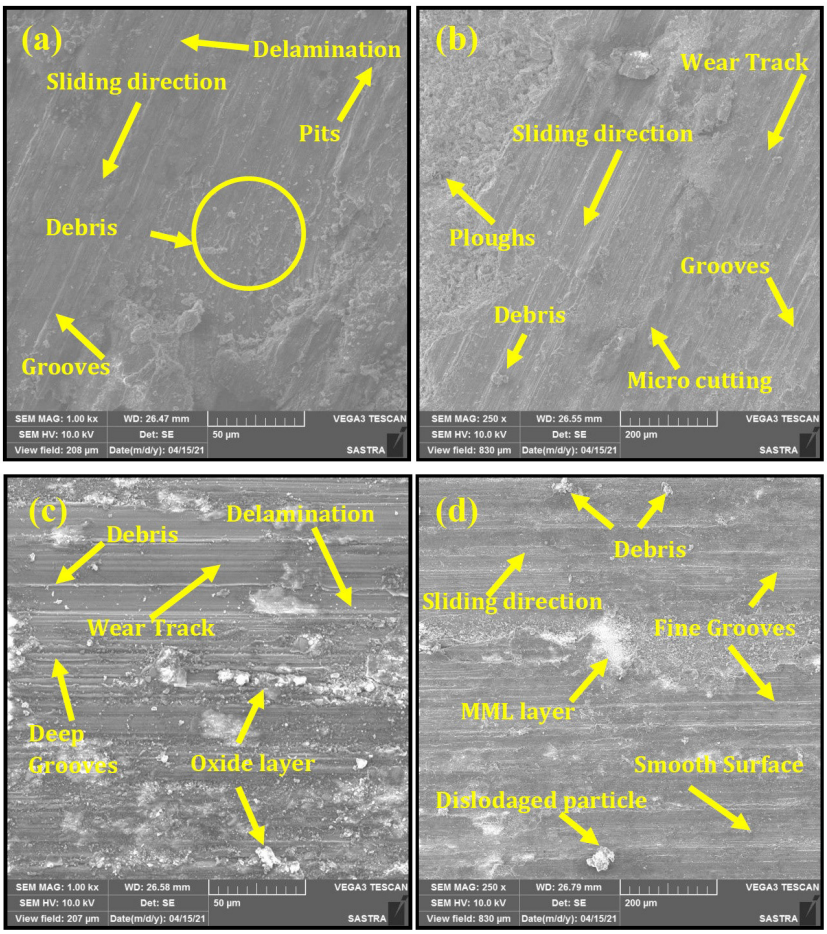


**Figure 10.** SEM images of worn surface of ZK60A Mg alloy-TiN composites (a) 0 wt. %, (b) 4 wt. %, (c) 8 wt. %, and (d) 12 wt. %.

## 4. Conclusions

1. In this research work, ZK60A Mg alloy reinforced with varying weight proportions (0, 4, 8 and 12wt.%) of TiN particulate composites was effectively synthesized via PM route.
2. The SEM images of proposed composites ensured that the inclusion of TiN particles was uniformly distributed into the matrix alloy.
3. The Rockwell hardness results showed that the addition of TiN particles significantly improved the hardness value and also it was noticed that 12 wt.% of TiN particulate reinforced composite gives the higher hardness value of 65.8 HRB.
4. Using a pin-on-disc instrument, a dry sliding wear test was used to examine the tribological behaviour of the produced composites. The tests were executed as per $L_{16}$ orthogonal layout by taking four control factors, namely 'R', 'P', 'V' and 'D.
5. Taguchi combined TOPSIS technique was used to identify the optimal conditions of parameters to produce composites with low WR and COF. The results stated that the optimum level of parameters found to be at 12 wt.% of 'R', 9.81 N of 'P', 5.24 m/s of 'V' and 1000 m of 'D', respectively.
6. ANOVA results confirmed that the addition of TiN content has the primary significant factor for controlling the WR and COF, followed by an applied load (P) having a contribution of 82.68% and 14.80%, respectively.
7. The worn surface morphology showed the micro cutting or pits, ploughs, delamination and the formation of oxide layer on the specimen surface in dry sliding conditions.

## 5. References


1. Zhou X, Zhang Z, Li X, Zhou L, Zhang X, Chen M. Microstructure and phase evolution characteristics of the in situ synthesis of TiC-reinforced AZ91D magnesium matrix composites. Materials. 2022;15(4):1278.
2. Mehra D, Mahapatra MM, Harsha SP. Optimizations of Abrasive wear analysis of RZ5/TiC in-situ composites: a statistical approach. Ind Lubr Tribol. 2019;71(9):1029-37.
3. Purohit R, Dewang Y, Rana RS, Koli D, Dwivedi S. Fabrication of magnesium matrix composites using powder metallurgy process and testing of properties. Mater Today Proc. 2018;5(2):6009-17.
4. Loganathan P, Gnanavelbabu A, Rajkumar K. Influence of ZrB2/hBN particles on the wear behaviour of AA7075 composites fabricated through stir followed by squeeze cast technique. J Engineering Tribology. 2020;235:1-12.
5. Falcon Franco L, Bedolla Becerrila E, Lemus Ruiz J, Gonzalez Rodriguez JG. Wear performance of TiC as reinforcement of a magnesium alloy matrix composite. Compos, Part B Eng. 2011;42(2):275-9.
6. Aydin M, Findik F. Wear properties of magnesium matrix composites reinforced with $SiO_2$ particles. Ind Lubr Tribol. 2010;62(4):232-7.
7. Ozgun O, Ercetin A. Microstructural and mechanical properties of Cr-C reinforced Cu matrix composites produced through powder metallurgy method. Tr J Nature Sci. 2017;6:1-6.
8. Arora GS, Saxena KK, Mohammed KA, Prakash C, Dixit S. Manufacturing techniques for Mg-based metal matrix composite with different reinforcements. Crystals. 2022;12(7):945.
9. Sun S, Deng N, Zhang H, He L, Zhou H, Han B, et al. Microstructure and mechanical properties of AZ31 magnesium alloy reinforced with novel sub-micron vanadium particles by powder metallurgy. J Mater Res Technol. 2021;15:1789-800.
10. Ercetin A, Pimenov DY. Microstructure, mechanical, and corrosion behavior of $Al_2O_3$ reinforced Mg2Zn matrix magnesium composites. Materials. 2021;14(17):1-17.
11. Aatthisugan A, Razal Rose D, Jebadurai S. Mechanical and wear behaviour of AZ91D magnesium matrix hybrid composite reinforced with boron carbide and graphite. J Magnes Alloy. 2017;5(1):20-5.
12. Narayanasamy P, Selvakumar N. Tensile. Compressive and wear behaviour of self-lubricating sintered magnesium-based composites. Trans Nonferrous Met Soc China. 2017;27(2):312-23.
13. Dash D, Singh R, Samanta S, Rai RN. Influence of TiC on microstructure, mechanical and wear properties of magnesium alloy (AZ91D) matrix composites. J Sci Ind Res. 2020;79:164-9.
14. Meher A, Mahapatra MM, Samal P, Vundavilli P. Study on effect of TiB2 reinforcement on the microstructural and mechanical properties of magnesium RZ5 alloy based metal matrix composites. J Magnes Alloy. 2020;8(3):780-92.
15. Sunu Surendran KT, Gnanavelbabu A. Tribological behaviour of AZ91D/ultra-hightemperature ceramic composites at room and elevated temperatures. P I Mech Eng J. 2021;236:1-16.
16. Satish J, Satish KG. Preparation of magnesium metal matrix composites by powder metallurgy process. IOP Conf Series Mater Sci Eng. 2018;310:012130.
17. Mehra D, Mahapatra MM, Harsha SP. Optimizations of RZ5-TiC magnesium matrix composite wear parameters using Taguchi approach. Ind Lubr Tribol. 2018;70(5):907-14.
18. Sathish S, Anandakrishnan V, Sankaranarayanan S, Gupta M. Optimization of wear parameters of Magnesium metal-metal composite using Taguchi and GA technique. J Tribol. 2019;23:76-89.
19. Selvam B, Marimuthu P, Narayanasamy R, Anandakrishnan V, Tun KS, Gupta M, et al. Dry sliding wear behaviour of zinc oxide reinforced magnesium matrix nano-composites. Mater Des. 2014;58:475-81.
20. Lim CYH, Lim SC, Gupta M. Wear behaviour of $SiC_p$-reinforced magnesium matrix composites. Wear. 2003;255(1-6):629-37.
21. Mahesh L, Reddy S, Vinyas M. The study of microstructure and wear behaviour of titanium nitride reinforced aluminium composites. AIP Conf Proc. 2020;2204:040014.
22. Sathish S, Anandakrishnan V, Sankaranarayanan S, Gupta M. Optimization of wear parameters of Mg-(5.6Ti13Al)-2.5B4C composite. Ind Lubr Tribol. 2020;72:503-8.
23. Tarasasanka C, Snehita K, Ravindra K, Sameerkumar D. Optimization of dry sliding wear properties ofAZ91E/ nano $Al_2O_3$ reinforced metal matrix composite with grey relational analysis. Int J Eng Sci. 2019;11:41-8.
24. Shen M, Zhu X, Han B, Ying T, Jia J. Dry sliding wear behaviour of AZ31 magnesium alloy strengthened by nanoscale SiCp. J Mater Res Technol. 2022;16:814-23.
25. Alam MT. Physical, corrosion and microstructural analysis of A356/SiC nanocomposites fabricated through stir casting process. Mater Sci Forum. 2021;1034:73-86.
26. Khan MM, Dey A, Hajam MI. Experimental investigation and optimization of dry sliding wear test parameters of aluminum based composites. Silicon. 2022;14(8):4009-26.
27. Alagarsamy SV, Ravichandran M. Parametric studies on dry sliding wear behaviour of A1-7075 alloy matrix composite using S/N ratio and ANOVA analysis. Mater Res Express. 2020;7(1):1-17.
28. Raveendran P, Alagarsamy SV, Chanakyan C, Meignanamoorthy M, Ravichandran M, Sakthivelu S. A hybrid approach for prediction of machining performances of glass fiber reinforced plastic (epoxy) composites. Surf Topogr. 2021;9:1-12.
29. Girish BM, Satish BM, Sarapure S, Basawaraj. Optimization of wear behavior of magnesium alloy AZ91 hybrid composites using taguchi experimental design. Metall Mater Trans, A Phys Metall Mater Sci. 2016;47(6):3193-200.

30. Sai Ram YNV, Tara Sasanka C, Prabakaran J. Optimization of dry-sliding wear parameters on lanthanum hexa aluminate reinforced magnesium AZ91E composites using grey relation analysis. Nano Hybrid Composites. 2022;35:55-73.
31. Ayyanar S, Gnanavelbabu A, Rajkumar K, Loganathan P, Vishal K. Investigation on microstructure and tribological performance of zirconium boride reinforced AZ91D magnesium alloy: effect of processing routes. Proc Inst Mech Eng, C J Mech Eng Sci. 2023;237(3):692-707.
32. Balaji S, Maniarasan P, Alagarsamy SV, Raveendran P, Mohanavel V. Optimization and prediction of tribological behaviour of Al-Fe-Si alloy based nano grains refined composites using taguchi with response surface methodology. J Nanomater. 2022.
33. Alagarsamy SV, Balasundaram R, Ravichandran M, Mohanavel V, Karthick A, Devi S. Taguchi approach and decision tree algorithm for prediction of wear rate in zinc oxide-filled AA7075 matrix composites. Surf Topogr. 2021;9(3):035005.